

Computational Study of Flow Interactions in Coaxial Rotors

Seokkwan Yoon, Henry C. Lee, and Thomas H. Pulliam
NASA Ames Research Center, Moffett Field, California 94035

I. Introduction

Although the first idea of coaxial rotors appeared more than 150 years ago¹, most helicopters have used single main-rotor/tail-rotor combination. Since reactive moments of coaxial rotors are canceled by contra-rotation, no tail rotor is required to counter the torque generated by the main rotor. Unlike the single main rotor design that distributes power to both main and tail rotors, all of the power for coaxial rotors is used for vertical thrust. Thus, no power is wasted for anti-torque or directional control. The saved power helps coaxial rotors reach a higher hover ceiling than single rotor helicopters. Another advantage of coaxial rotors is that the overall rotor diameter can be reduced for a given vehicle gross weight because each rotor provides a maximum contribution to vertical thrust to overcome vehicle weight.² However, increased mechanical complexity of the hub has been one of the challenges for manufacturing coaxial rotorcraft. Only the Kamov Design Bureau of Russia had been notably successful in production of coaxial helicopters until Sikorsky built X2, an experimental compound helicopter.

Recent developments in unmanned aircraft systems and high-speed rotorcraft have renewed interest in the coaxial configuration. Multi-rotors are frequently used for small electric unmanned rotorcraft partly due to mechanical simplicity. The use of multiple motors provides redundancy as well as cost-efficiency. The multi-rotor concept has rarely been used until recently because of its inherent stability and control problems. However, advances in inexpensive electronic flight control systems have opened the floodgates for small drones using multi-rotors. Coaxial rotors have started to appear in some multi-rotor configurations.

Small coaxial rotors have often been designed using a hundred year old approach that is “sketch, build, fly, and iterate.” In that approach, there is no systematic way to explore trade-offs or determine logical next steps.³ It is neither possible to account for multiple real-world constraints up front in design nor possible to know what performance is possible with a given design. Since unmanned vehicles are sized and optimized for the particular mission, a modern low-fidelity conceptual design and sizing tool that has been used for the design of large helicopters can be used for design of small coaxial rotorcraft.

However, unlike most helicopters with single main rotor, the interactions between the upper and lower rotors emerge as an important factor to consider in design because an increase in performance of a multi-rotor system is not proportional to the number of rotors. Interference losses and differences in thrusts between the upper and lower rotors were investigated by theoretical methods⁴ as well as a computational fluid dynamics (CFD) method^{5,6} using the Reynolds-Averaged Navier-Stokes (RANS) equations. In this work, hybrid turbulence models are used to investigate the physics of interactions between coaxial rotors and a fuselage that are not well understood.

Present study covers not only small-scale drones but also large-scale coaxial rotors for heavy-lifting missions. Considering the recently proposed FAA drone rules that require the flight only in visual line-of-sight, a large multi-rotor might be used as an airborne carrier for launch and recovery of unmanned aircraft systems with a human operator onboard. For applications to civil operations, their aerodynamic performance and noise levels need to be assessed. Noise is one of the largest limiting factors to rotorcraft operations in urban area. Since the high-frequency noise of multi-rotors may increase the annoyance, noise may turn out to be a key issue that must be addressed for market acceptability. One of the objectives of the present work is to study the effects of inter-rotor spacing and collectives on the performance, efficiency, and acoustics of coaxial rotor systems.

II. Numerical Approach

Accurate prediction of rotorcraft performance in hover continues to be challenging for CFD. Flows are inherently complex because a rotor blade can encounter its own tip vortex and the tip vortices of other blades. The distance from the rotor to the far-field boundary has a significant effect on the figure of merit (FM) prediction. The asymptotic FM is reached when the far-field boundary is located about fifteen to twenty rotor radii away from the rotor.⁷ Also, it often requires twenty to thirty revolutions for a running mean of the FM to reach a quasi steady state even in free air.

OVERFLOW solves the Reynolds-Averaged Navier-Stokes (RANS) equations on structured overset grids. The current time-accurate approach consists of an inertial coordinate system where near-body (NB) curvilinear O-grids (rotor blades and hub) rotate through a fixed off-body (OB) Cartesian grid system. This study employs the medium-sized XV-15 isolated rotor grid system used in Ref. 7 and Ref. 8. A uniformly spaced OB Cartesian grid surrounds the rotor blades and hub and resolves the rotor wake region of interest. Coarser “brick-grids” efficiently expand the grid system to the far field, where each successive brick grid is twice as coarse as its previous neighbor. The XV-15 isolated rotor consists of three highly twisted rotor blades and a simplified hub. Each rotor blade consists of three O-grids, one for the main rotor blade and two “cap-grids” for the inboard and outboard tips. The grid spacing normal to solid surfaces maintains $y^+ < 1$. The resolved wake region has uniform grid spacing of 10% c_{tip} (rotor blade tip chord length). Care is taken to make sure the NB grid spacing is similar to the OB grid spacing where the grids overlap.

A notional contra-rotation coaxial rotor system was constructed by incorporating two sets of the above mentioned XV-15 rotor grid system. The clockwise rotor was generated by mirroring the XV-15 isolated (counter-clockwise rotating) rotor. The coaxial rotor system results in approximately 67 - 86 million grid points depending on the inter-rotor spacing. The collective for all the rotors was set to 10.04 degrees, and the precone angle was set to 1.5 degrees.

The tandem coaxial rotor vehicle system incorporates two coaxial rotor systems and a fuselage body. The XV-15 blade rotors are translated into their respective locations. The fuselage currently is based off of an arbitrary shape, but will be changed to the Common Research Model’s fuselage¹⁵ to better resemble a realistic geometry. The fuselage consists of 4 grids covering the nose, port and starboard portion of the fuselage, and a fuselage end cap. The resulting grid system has 238 grids, with 52 NB grids, and approximately 142 million grid points.

OVERFLOW solves the Navier-Stokes equations using finite differences with a variety of numerical algorithms and turbulence models.⁹ Up to 6th-order spatial accuracy for inviscid fluxes, up to 7th-order artificial dissipation, and 2nd-order time accuracy are available.¹⁰ In this study, the Pulliam-Chaussee¹¹ diagonal central difference algorithm is used with the 5th-order spatial differencing option. Dual time-stepping is used to advance the simulation in time with 2nd-order time accuracy. The physical time step corresponds to 0.25 degrees rotor rotation, together with 30 dual-time sub-iterations. This typically provides for a 2.5 orders of magnitude drop in sub-iteration residual. This numerical approach and time step was previously validated for similar isolated rotor flows.⁸ In order to reduce the computational time required for a converged solution, the first 1,440 steps employ a time step of 2.5 deg, i.e., 10 rotor revolutions. The time step is then reduced to 0.25 deg, when 1,440 steps now correspond to one rotor revolution.

Rotorcraft simulations using the Detached Eddy Simulation¹² (DES) model have been successfully performed to capture the FM within experimental error. An alternative approach is to turn off the production terms in the off-body grid wake region. The Laminar Off-Body (LOB) model¹³ assumes that the turbulent eddy viscosity that is generated elsewhere, e.g., the rotor blades, can still convect, but not be produced, dissipate, or diffuse. Both DES and LOB models produce accurate solutions and their FM results are comparable.^{7,8}

The RANS equations require a closure by modeling the Reynolds stress. The one-equation Spalart-Allmaras¹⁴ (SA) RANS model is one of the models commonly used to compute the turbulent eddy viscosity (TEV) using the Boussinesq approximation.

III. Results

The XV-15 rotors have been used for computational simulations of coaxial rotor systems in this study. The diameter of the XV-15 rotor is 25 ft. The Mach number at the rotor tip is 0.6902, the Reynolds number 4.925 million based on the chord length of the rotor blade, and temperature 59.03 deg F. Preliminary results have been obtained using the LOB model for the OB grids. The final manuscript will include the solutions using the DES model for the OB grids to compare the two turbulence models.

Figure 1 shows Q-criterion for contra-rotating coaxial rotors at multiple viewing angles. The inter-rotor spacing is 0.25 of the rotor diameter (D). The collective is set to 10° for both upper and lower rotors in this case. Figure 1a shows that the wake from the upper rotor contracts inward while the lower rotor exhibits turbulent flows in its wake. A close look in Fig. 1b shows the interactions between the lower rotor blades and the trailing vortices of the upper rotor.

The design of an efficient coaxial rotor system requires an accurate assessment of aerodynamic interferences between the rotors. The momentum theory suggests that the minimum induced losses for coaxial rotors is attained when the lower rotor operates in the fully developed slipstream of the upper rotor and at equal and opposite torque to the upper rotor.² A CFD result⁶ shows that the upper rotor thrust increases with the inter-rotor spacing whereas the lower rotor thrust decreases as the inter-rotor spacing increases. Vorticity magnitude contours in Fig. 2 shows the effect of the inter-rotor spacing on coaxial rotor flows. The inter-rotor spacing started with 1.0D and reduced to 0.5D and 0.25D. The inter-rotor spacing is further reduced to 0.15D in Fig. 3a and the result is compared to an isolated rotor. When the inter-rotor spacing is large as in Fig. 2a or 2b, the interference effect might be relatively small. However, the lower rotor wake becomes highly turbulent and hence reduces the thrust. When the inter-rotor spacing is small as in Fig. 2c or Fig 3a, the upper rotor vortices are preserved inside the lower rotor wake and the lower rotor thrust increases. Although not shown in the abstract, the overall thrust seems to increase as the inter-rotor spacing decreases because the rate of increase in the lower rotor thrust is higher than the rate of decrease in the upper rotor thrust.

Figure 4a and 4b show downward velocity components for coaxial rotors with the inter-rotor spacing 1.0D and 0.25D and they are compared to an isolated rotor in Fig. 4c. The color map is inverted here, so red indicates high downward velocities while blue upward velocity zones. The upper rotor wake appears to convect downward at a slower rate than the lower rotor.

Figure 5 compares pressure fluctuations for coaxial rotors and an isolated rotor. Stronger pressure waves in the coaxial rotors in Fig. 5a than in the isolated rotor in Fig. 5b suggest that the coaxial rotors might be noisier than the isolated rotor. Figure 6 shows vorticity magnitude and Q-criterion for tandem coaxial rotors. Both the vertical inter-rotor spacing and the horizontal rotor separation distance are 1.0D. Because of the interaction of two coaxial rotor systems, the lower rotor wakes pulled close to each other. Figure 6b also shows the interaction of pressure waves between two coaxial rotor systems.

In order to investigate multiple rotor interactions for a full coaxial rotorcraft, a fuselage has been added to the tandem coaxial rotors. The vertical inter-rotor spacing and the horizontal rotor separation distance are 0.25D and 0.3D respectively. Figure 7 shows Q-criterion and surface pressure. Pressure on a coordinate plane is shown as well. The interactions between coaxial rotors and the fuselage create complex vortical flows. Especially, the vortices between the two coaxial rotor systems are stretched and the upper and lower parts move in opposite directions.

The final manuscript will include the effect of different collectives for the upper and lower rotors on aerodynamic performance and efficiency.

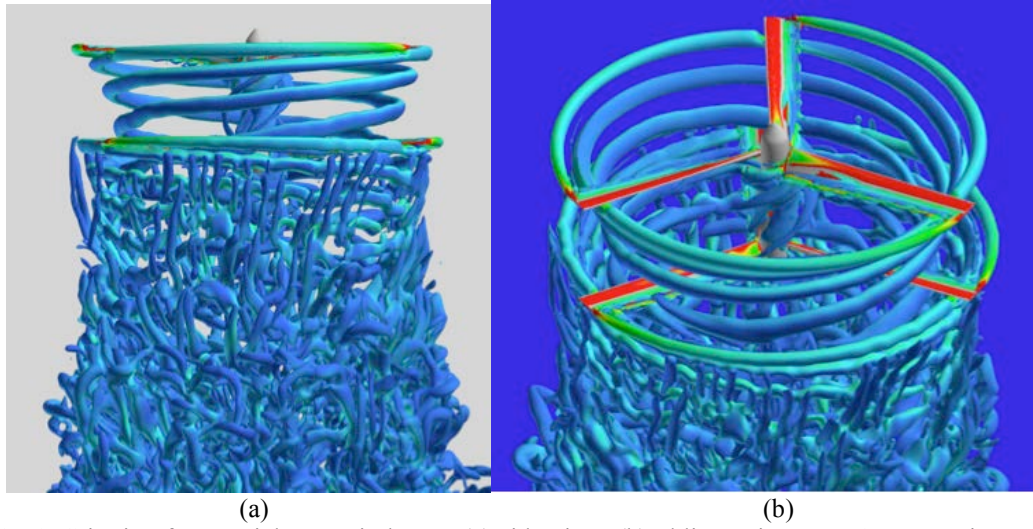


Figure 1. Q-Criterion for coaxial rotors in hover. (a) side view, (b) oblique view, XV-15 rotors, inter-rotor spacing = $0.25D$, $M_{tip}=0.69$, $Re_{Ctip}=4.9$ million, $\theta=10^\circ$

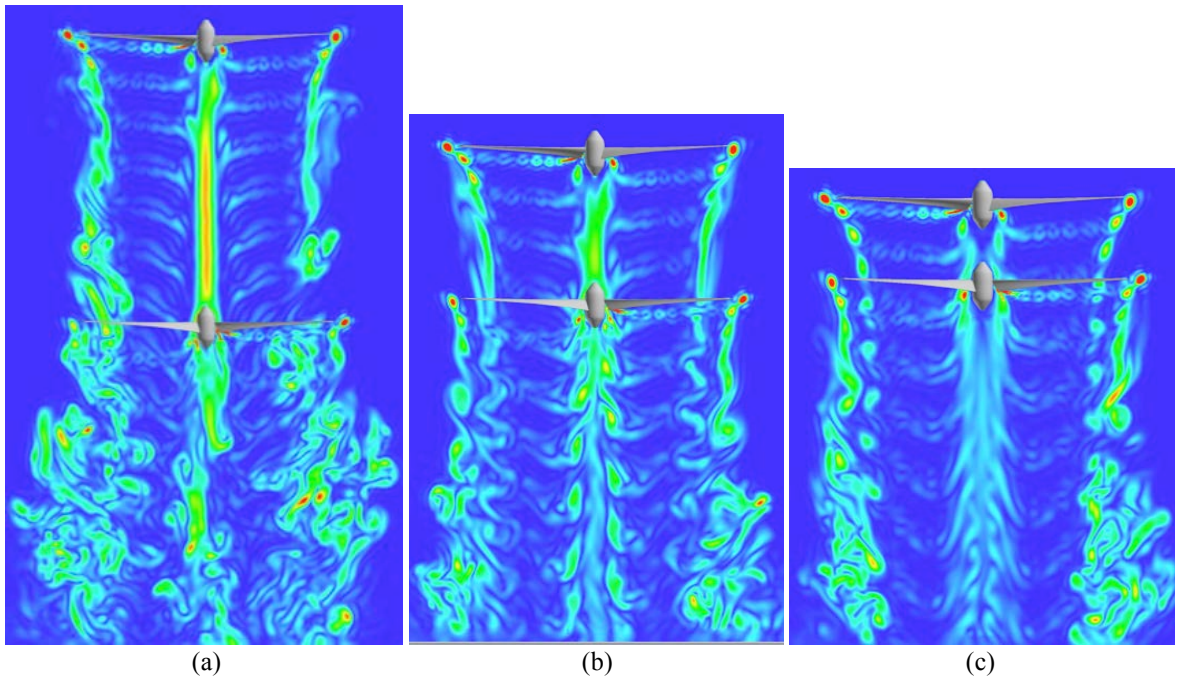


Figure 2. Vorticity magnitude for coaxial rotors in hover. (a) inter-rotor spacing= $1.0D$, (b) inter-rotor spacing= $0.5D$, (c) inter-rotor spacing= $0.25D$, XV-15 rotors, $M_{tip}=0.69$, $Re_{Ctip}=4.9$ million, $\theta=10^\circ$.

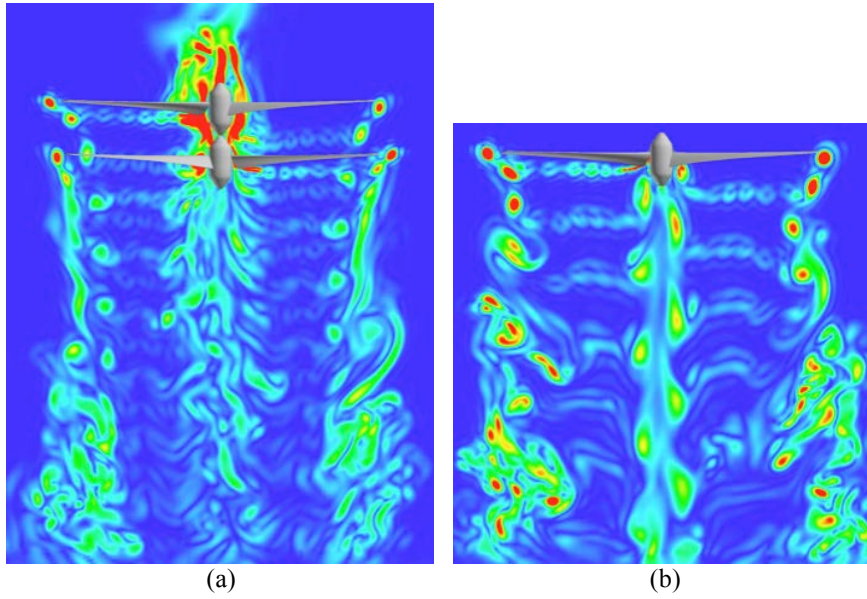


Figure 3. Vorticity magnitude for coaxial rotors and an isolated rotor in hover. (a) inter-rotor spacing=0.15D, (b) isolated rotor, XV-15 rotors, $M_{tip}=0.69$, $Re_{Ctip}=4.9$ million, $\theta=10^\circ$.

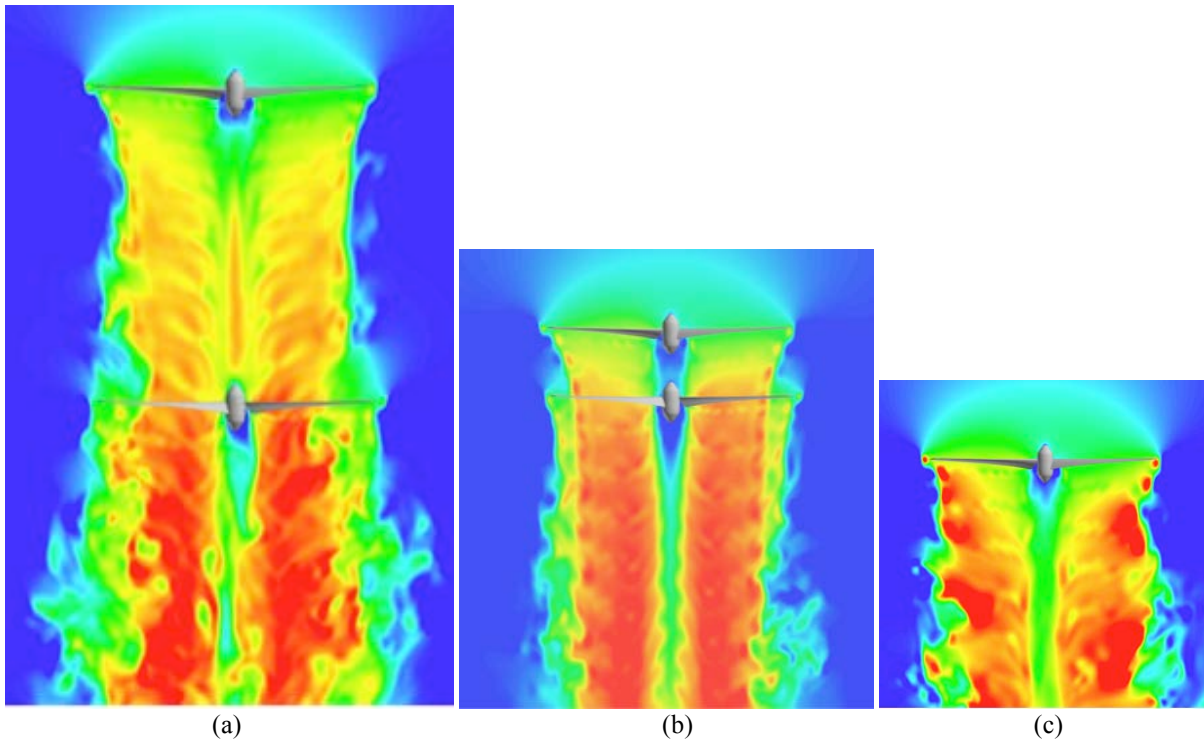


Figure 4. W-velocity (inverted) for coaxial rotors and an isolated rotor in hover. (a) inter-rotor spacing=1.0D, (b) inter-rotor spacing = 0.25D, (c) isolated rotor, XV-15 rotors, $M_{tip}=0.69$, $Re_{Ctip}=4.9$ million, $\theta=10^\circ$.

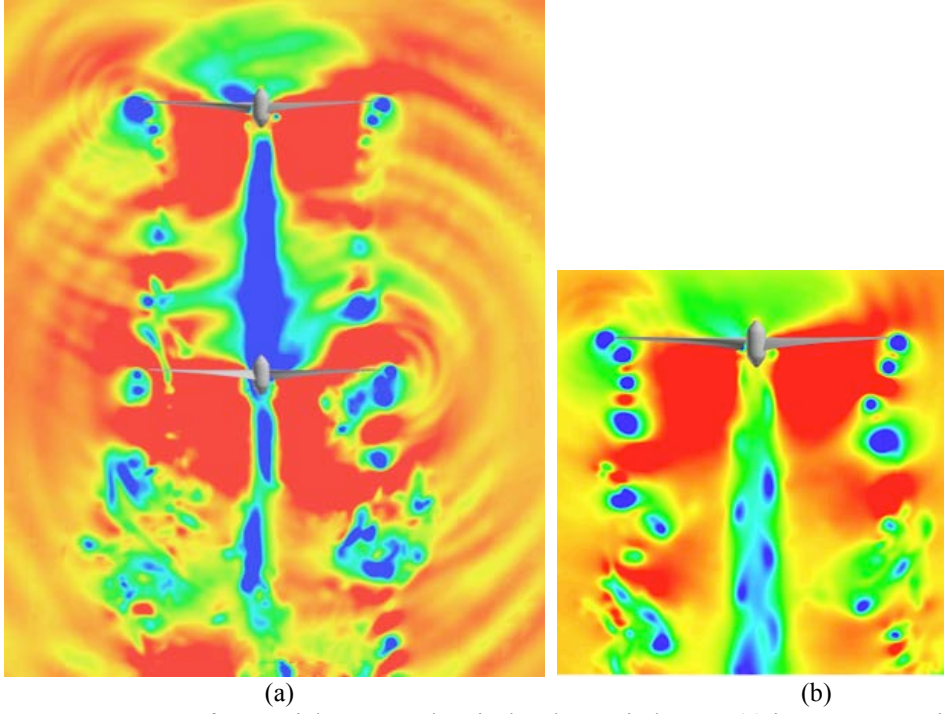


Figure 5. Pressure for coaxial rotors and an isolated rotor in hover. (a) inter-rotor spacing = 1.0D, (b) isolated rotor, XV-15 rotors, $M_{tip}=0.69$, $Re_{Ctip}=4.9$ million, $\theta=10^\circ$.

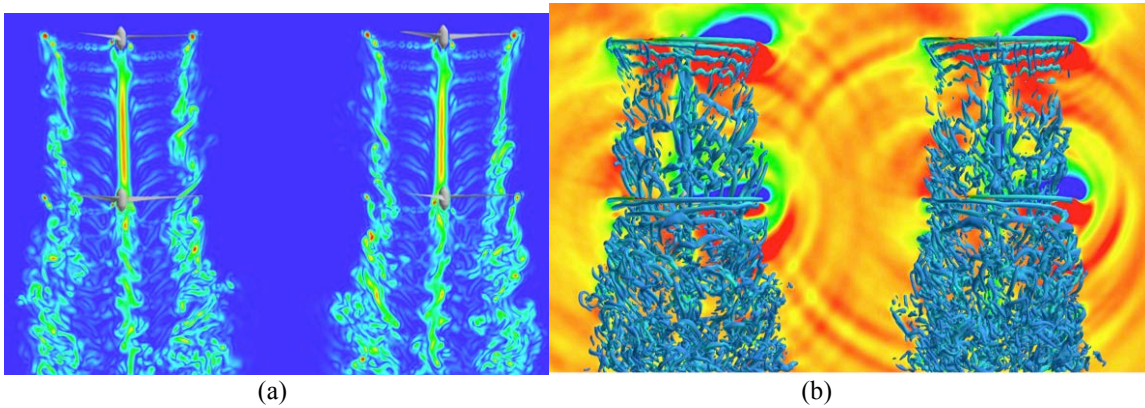


Figure 6. (a) Vorticity magnitude for tandem coaxial rotors in hover. (b) Q-Criterion and pressure. XV-15 rotors, inter-rotor spacing = 1.0D, rotor separation distance = 1.0D, $M_{tip}=0.69$, $Re_{Ctip}=4.9$ million, $\theta=10^\circ$.

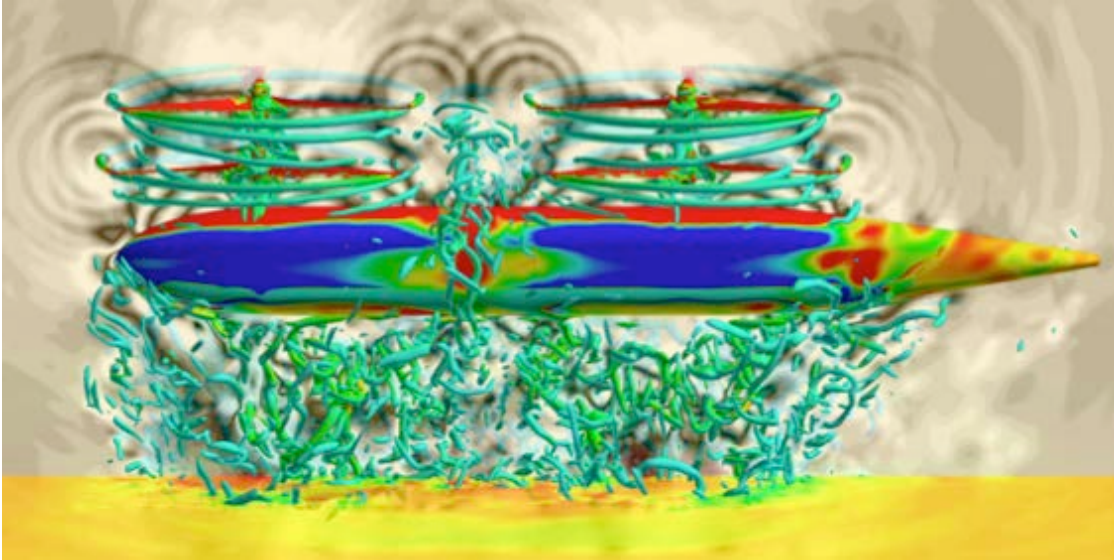


Figure 7. Q-Criterion and pressure for tandem coaxial rotors with a fuselage in hover. XV-15 rotors, inter-rotor spacing = 0.25D, rotor separation distance = 0.3D, $M_{tip}=0.69$, $Re_{Ctip}=4.9$ million, $\theta=10^\circ$.

References

- ¹Coleman, C. P., "A Survey of Theoretical and Experimental Coaxial Rotor Aerodynamic Research," NASA TP 3675, NASA Ames Research Center, 1997.
- ²Leishman, J. G. and Ananthan, S., "Aerodynamic Optimization of a Coaxial Proprotor," The 62nd AHS Annual Forum, May 2006.
- ³Theodore, C., "Vertical Lift Hybrid Autonomy," The VLHA Meeting, NASA Ames Research Center, May 2015.
- ⁴Syal, M. and Leishman, J. G., "Aerodynamic Optimization Study of a Coaxial Rotor in Hovering Flight," *Journal of the American Helicopter Society*, 57, 042003, 2012.
- ⁵Lakshminarayan, V. K. and Baeder, J. D., "High-Resolution Computational Investigation of Trimmed Coaxial Rotor Aerodynamics in Hover," *Journal of the American Helicopter Society*, 54, 042008, 2009.
- ⁶Lakshminarayan, V. K. and Baeder, J. D., "Computational Investigation of Microscale Coaxial-Rotor Aerodynamics in Hover," *Journal of Aircraft*, Vol. 47, No. 3, May-June 2010.
- ⁷Yoon, S., Pulliam, T. H., and Chaderjian, N. M., "Simulations of XV-15 Rotor Flows in Hover Using OVERFLOW," The 5th Decennial AHS Aeromechanics Specialists' Conference, San Francisco, Jan. 2014.
- ⁸Yoon, S., Chaderjian, N. M., Pulliam, T. H., and Holst, T. L., "Effect of Turbulence Modeling on Hovering Rotor Flows," The 45th AIAA Fluid Dynamics Conference, Dallas, Texas, June 2015.
- ⁹Nichols, R., Tramel, R., and Buning, P., "Solver and Turbulence Model Upgrades to OVERFLOW2 for Unsteady and High-Speed Flow Applications," AIAA Paper 2006-2824, June 2006.
- ¹⁰Pulliam, T. H., "High Order Accurate Finite-Difference Methods: as seen in OVERFLOW," AIAA Paper 2011-3851, June 2011.
- ¹¹Pulliam, T. H., and Chaussee, D. S., "A Diagonal Form of an Implicit Approximate-Factorization Algorithm," *Journal of Computational Physics*, Vol. 39, No. 2, 1981, pp. 347-363.
- ¹²Spalart, P. R., W-H. Jou, Strelets, M., and Allmaras, S. R., "Comments on the Feasibility of LES for Wings and on a Hybrid RANS/LES Approach," *Advances in DNS/LES*, Greyden Press, 1997, pp. 137-147.

¹³Potsdam, M. and Pulliam, T. H., "Turbulence Modeling Treatment for Rotorcraft Wakes," AHS Aeromechanics Specialists Meeting, Jan. 2008.

¹⁴Spalart, P. R. and Allmaras, S. R., "A One-Equation Turbulence Model for Aerodynamic Flows," AIAA Paper 1992-0439, Jan. 1992.

¹⁵Vassberg, J. C., DeHaan, M. H, Rivers, S. M., and Wahls, R. A., "Development of a Common Research Model for Applied CFD Validation Studies," AIAA Paper 2008-6919, August 2008